
Stratified Hazard Sampling: Minimal-Variance Event Scheduling for CTMC/DTMC Discrete Diffusion and Flow Models

Seunghwan Jang¹ SooJean Han¹

Abstract

CTMC/DTMC-based discrete generative models, including uniform-noise discrete diffusion (e.g., D3PM/CTDD) and discrete flow matching, enable non-autoregressive sequence generation by repeatedly replacing tokens through a time-inhomogeneous Markov process. Inference is typically implemented with step-based simulation: each token decides to jump via independent Bernoulli (or categorical) draws at every discretization step. Under uniform-noise initialization, where self-correction requires multiple edits per position, these independent decisions induce substantial variance in both the number and timing of edits, leading to characteristic failure modes such as under-editing (residual noise) or over-editing (cascading unnecessary substitutions), decreasing reproducibility.

We propose *Stratified Hazard Sampling* (SHS), a drop-in and hyperparameter-free inference principle for any sampler that admits a stay-vs.-replace decomposition. SHS models per-token edits as events driven by cumulative hazard (CTMC) or cumulative jump mass (DTMC) and places events by stratifying this cumulative quantity: with a single random phase per position, a token jumps whenever its accumulated hazard crosses unit-spaced thresholds. This preserves the expected number of jumps while achieving the minimum possible variance among unbiased integer estimators (bounded by $1/4$), without altering per-jump destination sampling and thus retaining multimodality. We also introduce a phase-allocation variant for blacklist-style lexical constraints that prioritizes early edits at high-risk positions to mitigate late-masking artifacts.

1. Introduction

Non-autoregressive generation for high-dimensional discrete data (e.g., text, code) is a promising approach that can significantly reduce inference latency by updating all tokens

in parallel. Recently, a growing family of methods has re-cast discrete generation as a time-inhomogeneous Markov process that transports an easy prior p_0 to the data distribution p_1 . This includes discrete diffusion models defined on a discrete time grid (DTMC; e.g., D3PM), continuous-time Markov jump process formulations (CTMC; e.g., CTDD), and discrete flow matching variants. Despite differences in training objectives, their inference procedures share a common primitive: at each time (or step), each position either stays put or is replaced according to a learned categorical kernel, with a time-dependent mass/rate controlling how often replacements occur.

The core focus of this paper is on how the choice of initialization (prior) fundamentally alters the complexity and variance structure of the sampling trajectories. Consider mask-start initialization, also known as absorbing-state initialization (Austin et al., 2021; Campbell et al., 2022), which begins with all tokens as [MASK] and permits only unmasking: each position transitions monotonically from [MASK] to a token exactly once, resulting in highly simplistic sampling paths. This offers advantages in training and inference stability, as well as straightforward implementation. Yet, this monotonic unmasking-only structure inherently disallows natural re-jumps to “refine” already selected tokens. To enable revisions, one must insert a re-masking trick where we revert positions to [MASK] and then unmask again, which introduces inefficient extra transitions, model evaluations, and conflicts with the original monotonic CTMC design. In essence, this approach resembles an autoregressive (AR) process with parallel or randomized update orders, where each position is finalized only once.

In contrast, uniform-noise start (Austin et al., 2021; Lou et al., 2024; Schiff et al., 2025) (initializing each position with a random token) allows the timing and frequency of jumps at each position to be contextually determined based on the current sequence, naturally enabling multiple jumps. This provides a self-correction capability, where misplaced tokens can be iteratively refined to better fit the evolving context. However, this flexibility comes at the cost of increased trajectory complexity, amplifying uncertainties in jump counts and timings. In standard time-step approximations, this manifests as frequent failure modes at the tails. There are two common types of failure modes that

occur. *Under-editing* (too few jumps) occurs when insufficient substitutions occur, leaving residual noise or local inconsistencies, and preventing full integration of contextual information before the process effectively halts. Conversely, *over-editing* (too many jumps) occurs when excessive substitutions cascade, disrupting even coherent segments and leading to repeated unnecessary edits, resulting in repetitions or distortions rather than convergence.

The goal of this paper is to preserve the expressive power of multiple jumps (i.e., self-correction) inherent to uniform-noise-start CTMC discrete language models (LMs), while structurally eliminating unnecessary sampler variance—particularly the high variance in jump counts and event timings induced by the sampler. To achieve this, we propose *Stratified Hazard Sampling (SHS)*, which models jumps as a non-homogeneous Poisson process (NHPP) and uses the cumulative hazard $S(t) = \int_0^t \lambda(s) ds$ to stratify event placement in this space. SHS triggers jumps when the cumulative hazard $S(t)$ crosses integer boundaries offset by a random $\theta \sim \text{Uniform}(0, 1)$. Unlike prior works (Austin et al., 2021; Campbell et al., 2022; Lou et al., 2024; Schiff et al., 2025; Gat et al., 2024), which used probabilistic coin flips at fixed time steps to trigger the jumps, SHS preserves the expected jump count while bounding the jump count variance to a theoretical minimum (at most $1/4$; see Appendix B). Consequently, SHS mitigates the long-tail waiting times and “sampling luck” that are especially pronounced in uniform-noise starts, simultaneously suppressing under- and over-editing, and enabling more stable, reproducible sampling even with fewer neural function evaluations (NFEs).

In addition to variance reduction, we propose a simple yet effective *lexically constrained safety* mechanism built on our SHS approach. We focus on blacklist-based lexical constraints, where users explicitly specify a set of prohibited tokens and the sampler enforces this constraint via token-level filtering; this approach is attractive because it is transparent, controllable, and can provide hard safety guarantees without retraining (Hokamp & Liu, 2017; Post & Vilar, 2018; Hu et al., 2019; Gehman et al., 2020). However, naively masking and renormalizing prohibited tokens at each local transition generally deviates from the desired conditional distribution ($p(x \mid c)$), often causing “late masking” artifacts when high-risk positions are corrected only after other tokens have already adapted to an unsafe context. Leveraging SHS’s hazard-space event scheduling method described in the previous paragraph, we bias jump timing so that positions with high violation risk are more likely to jump earlier, thereby resolving unsafe candidates sooner and reducing the mismatch to the conditional target distribution.

2. Preliminaries

2.1. CTMC/DTMC-based Discrete Generative Models

Let \mathcal{V} be a vocabulary, N the sequence length, and denote a sequence as $x = (x_1, \dots, x_N) \in \mathcal{V}^N$. We consider a continuous-time generative process $(X_t)_{t \in [0, 1]}$ with terminal distribution $p_1(x)$ and an initial distribution p_0 (often easy to sample, e.g., uniform or masked tokens). Many non-autoregressive discrete generative models can be expressed as a time-inhomogeneous Markov process on \mathcal{V}^N . We focus on the common *single-site replacement* structure (Austin et al., 2021; Campbell et al., 2022; Gat et al., 2024) where, at each (continuous or discrete) time, each position either stays unchanged or is replaced by a new token.

CTMC formulation. A time-inhomogeneous continuous-time Markov chain (CTMC) is specified by a generator Q_t . For each position i we define an *escape rate* $\lambda_i(t, x) \geq 0$ and a *destination distribution* $q_{t,i}(\cdot \mid x) \in \Delta(\mathcal{V})$. Let $x^{(i \leftarrow v)}$ denote the sequence obtained from x by replacing x_i with v . We parameterize off-diagonal rates as

$$Q_t(x^{(i \leftarrow v)} \mid x) = \lambda_i(t, x) q_{t,i}(v \mid x), \quad v \neq x_i, \quad (1)$$

and set $Q_t(x \mid x) = -\sum_i \lambda_i(t, x)$. This local CTMC view subsumes continuous-time discrete diffusion models (e.g., CTDD) and flow-based formulations (e.g., DFM) whenever their one-step update admits a mixture-of-(stay vs. replace) forms.

DTMC formulation (discrete diffusion). A large class of discrete diffusion models is defined on a discrete time grid and specifies a time-inhomogeneous discrete-time Markov chain (DTMC) with a learned reverse kernel $P_{t_{k+1} \mid t_k}(\cdot \mid x)$. For single-site updates, we write the per-position kernel as a categorical distribution $P_{k,i}(\cdot \mid x) \in \Delta(\mathcal{V})$. Any categorical kernel admits a (stay vs. replace) decomposition:

$$\begin{aligned} p_{ik}(x) &= 1 - P_{k,i}(x_i \mid x), \\ q_{k,i}(v \mid x) &= \frac{P_{k,i}(v \mid x)}{p_{ik}(x)} \quad (v \neq x_i), \end{aligned} \quad (2)$$

where $p_{ik}(x) \in [0, 1]$ is the probability of changing token i at step k and $q_{k,i}$ is the destination distribution conditional on changing.

Unified jump-mass view. Both CTMC τ -leaping and DTMC categorical updates can be written in the same schematic form: at step k , draw a change indicator $B_{ik} \sim \text{Bernoulli}(p_{ik})$ and, if $B_{ik} = 1$, sample a new token from $q_{k,i}(\cdot \mid x)$. For CTMC Euler/ τ -leaping, $p_{ik} = h \lambda_i(t_k, x)$ (assuming $p_{ik} \leq 1$); for DTMC, p_{ik} is given by (2). Define

the cumulative hazard/jump mass

$$S_{i,k} = \sum_{j=0}^{k-1} p_{ij}, \quad S_{i,n} \approx \int_0^1 \lambda_i(t, X_t) dt \quad (3)$$

Under the standard step-based sampler, the total number of jumps at position i is $J_i = \sum_{k=0}^{n-1} B_{ik}$, a Poisson-binomial random variable with $\mathbb{E}[J_i] = \sum_k p_{ik}$ and $\text{Var}(J_i) = \sum_k p_{ik}(1 - p_{ik})$. This Poisson-binomial variance, amplified under uniform-noise initialization where multiple self-correction edits are required, is the sampler-induced variance targeted by SHS. For more general background on CTMCs, DTMCs, and their relationship, the reader is referred to standard probability references such as [Ross \(2023\)](#) and [Grimmett & Stirzaker \(2020\)](#).

2.2. Lexical Safety as Conditioning, and Why Naive Masking Is Biased

We formalize token-level censorship (blacklists) as a *hard lexical constraint*. Let $\mathcal{B} \subset \mathcal{V}$ be a set of forbidden tokens and define the *safe set* of sequences

$$\mathcal{A} = \{x \in \mathcal{V}^N : \forall i, x_i \notin \mathcal{B}\}. \quad (4)$$

The distribution we ideally want is the conditional terminal distribution

$$p_1(x | \mathcal{A}) = \frac{p_1(x) \mathbf{1}[x \in \mathcal{A}]}{\mathbb{P}_{p_1}(X_1 \in \mathcal{A})}. \quad (5)$$

Exact conditioning via Doob h -transform. For a Markov process, conditioning on a terminal event generally changes the dynamics at *all* intermediate times. Let

$$h_t(x) = \mathbb{P}(X_1 \in \mathcal{A} | X_t = x) \quad (6)$$

be the probability of eventual safety from state x at time $t \in [0, 1]$. The generator of the conditioned Markov dynamics can be expressed via a Doob h -transform ([Doob, 1957](#)):

$$Q_t^{(\mathcal{A})}(x, y) = Q_t(x, y) \frac{h_t(y)}{h_t(x)} \quad (y \neq x), \quad (7)$$

and diagonal entries chosen so rows sum to zero. An analogous h -transform exists for DTMC transition kernels ([Rogers & Williams, 2000](#)) and similarly alters both the step-wise move probabilities and the destination distribution via lookahead survival. Crucially, (7) reweights *both* (i) *which* transitions are taken and (ii) *how frequently* they are taken, according to global lookahead information encoded by h_t .

Naive masking creates error w.r.t. $p_1(x | \mathcal{A})$. A common censorship heuristic ([Gehman et al., 2020](#)) modifies only the *destination distribution* by

$$q_{t,i}^{\text{MASK}}(v | x) \propto q_{t,i}(v | x) \mathbf{1}[v \notin \mathcal{B}], \quad (8)$$

and keeps the same escape rates $\lambda_i(t, x)$. This “naive masking” approach defines a *different* generator $Q_t^{\text{MASK}}(x^{(i \leftarrow v)} | x) = \lambda_i(t, x) q_{t,i}^{\text{MASK}}(v | x)$, which in general does not match the Doob-transformed generator (7).

Naive masking (8) effectively approximates the true lookahead weight $h_t(\cdot)$ by a *binary* surrogate that only checks whether a *single-step proposal* is forbidden. However, the correct conditional dynamics depends on how a proposed update changes the *future probability of reaching \mathcal{A} by time 1*. Unless $h_t(y)/h_t(x) \equiv 1$ for all allowed transitions (a degenerate case), we have $Q_t^{\text{MASK}} \neq Q_t^{(\mathcal{A})}$, and the induced terminal distribution under repeated masked updates is biased relative to (5).

The mismatch is especially pronounced in settings where the initial distribution p_0 assigns substantial mass to unsafe tokens (e.g., uniform-noise initialization). Then $h_t(x)$ varies widely across intermediate states, and the correct conditional process would preferentially accelerate transitions that remove high-risk tokens early. Naive masking alone cannot reproduce this global reweighting, since it does not model h_t .

3. Related Works

3.1. Discrete Diffusion and CTMC Generative Models

Diffusion-style generative modeling has been extended to discrete spaces in several ways. Multinomial diffusion and related categorical constructions were studied by [Hoogendoorn et al. \(2021\)](#). D3PM ([Austin et al., 2021](#)) generalizes discrete diffusion by allowing structured transition matrices, including absorbing-state and nearest-neighbor corruptions, and demonstrates strong results on text and images. A fully continuous-time perspective that explicitly formulates both forward corruption and reverse generation as CTMCs was developed by [Campbell et al. \(2022\)](#), connecting discrete diffusion sampling to Markov jump process simulation techniques. More recently, Score Entropy Discrete Diffusion (SEDD) ([Lou et al., 2024](#)) learns the reverse jump rates by estimating probability ratios (concrete scores) with a scalable score-entropy objective. In parallel, [Schiff et al. \(2025\)](#) revisited uniform-noise diffusion language models (UDLM), deriving discrete classifier-free/classifier-based guidance and improved variational training bounds, which are particularly relevant for controllable generation settings where multiple edits per position are common.

Beyond diffusion, flow-based viewpoints for discrete data have recently emerged. Discrete Flow Matching (DFM) ([Gat et al., 2024](#)) proposes a discrete analogue of flow matching for high-dimensional categorical data and reports strong performance in language and code generation. Other contemporaneous work explores geometric and manifold-aware discrete flow formulations.

3.2. Iterative Masked-Token Refinement for Non-Autoregressive Generation

A parallel line of work studies iterative refinement with masked language models. Mask-Predict (Ghazvininejad et al., 2019) performs parallel decoding by repeatedly masking and regenerating low-confidence tokens. MaskGIT (Chang et al., 2022) introduces a confidence-based masking schedule for fast non-autoregressive synthesis, popularizing keep-the-most-confident refinement. For language modeling, several diffusion-inspired or simplex/continuous relaxations have been proposed, including DiffusionBERT (He et al., 2023), SSD-LM (Han et al., 2022), and continuous-time/continuous-space categorical diffusion formulations (Dieleman et al., 2022).

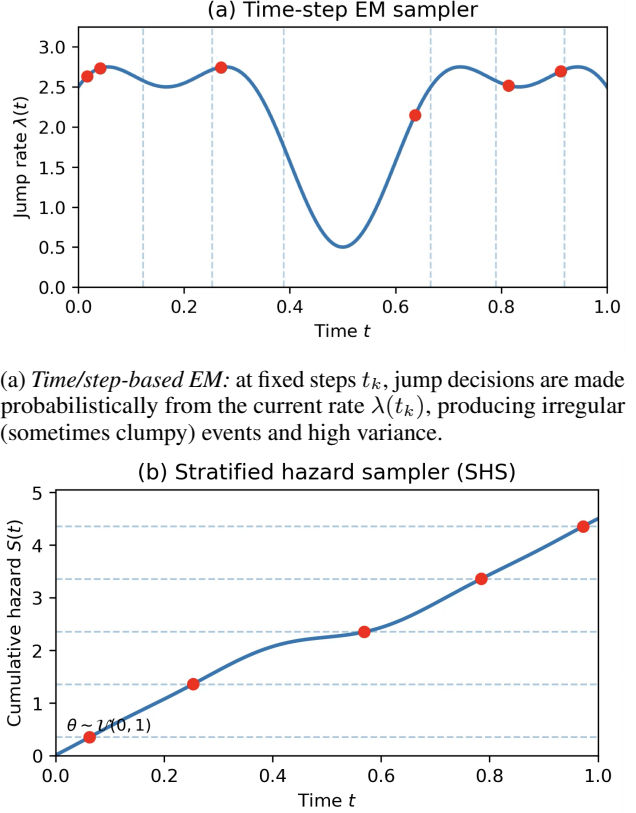
3.3. Constrained and Safe Generation via Lexical Constraints

Controlling generation with explicit lexical constraints has a long history in decoding-time algorithms. Grid Beam Search (Hokamp & Liu, 2017) and Dynamic Beam Allocation (Post & Vilar, 2018) enforce inclusion constraints efficiently, with later work improving batching and throughput (Hu et al., 2019). Finite-state and terminology-constrained decoding frameworks also appear in sequence generation and NMT settings.

In safety contexts, a common baseline is hard filtering or banning of disallowed tokens/phrases, but empirical evidence suggests that simple banned-word strategies are often insufficient as a complete safety solution, motivating principled approaches that better align with the desired conditional distribution (Gehman et al., 2020). Our work focuses on the *distributional* mismatch induced by naive censorship and how to reduce it within CTMC-based discrete generative modeling.

3.4. Simulation of Inhomogeneous Poisson Processes and Markov Jump Processes

Simulating CTMCs and non-homogeneous Poisson processes (NHPPs) is a classical topic. Thinning is a standard exact technique for NHPP simulation (Lewis & Shedler, 1979). Uniformization is widely used in Markov jump process inference and sampling, enabling algorithms that avoid expensive matrix exponentials while preserving correctness (Rao & Teh, 2013). These classical tools inform modern samplers for high-dimensional discrete diffusion and CTMC generative models, and motivate variance-reduction schemes tailored to discrete generative inference.



(a) *Time/step-based EM*: at fixed steps t_k , jump decisions are made probabilistically from the current rate $\lambda(t_k)$, producing irregular (sometimes clumpy) events and high variance.

(b) *Stratified Hazard Sampling*: accumulate cumulative hazard $S(t) = \int_0^t \lambda(s) ds$ and place unit-spaced boundaries with a single offset $\theta \sim U(0, 1)$. A jump occurs deterministically when $S(t)$ crosses $\theta + k$. This preserves the expected jump count while reducing variance to the minimal bound $\leq 1/4$.

Figure 1. Standard step-based sampler vs. SHS (ours).

4. Stratified Hazard Sampling

We propose *Stratified Hazard Sampling (SHS)*, adapting stratified event simulation to the *step-based* samplers used in CTMC/DTMC discrete generative models. SHS replaces the independent per-step change decisions $B_{ik} \sim \text{Bernoulli}(p_{ik})$ (Section 2) with a *single-phase* stratification in cumulative hazard/jump-mass space. Concretely, SHS maintains the cumulative mass $S_{i,k}$ from (3) and triggers a jump whenever $S_{i,k}$ crosses unit-spaced thresholds $\{\theta_i + m\}_{m \in \mathbb{Z}_{\geq 0}}$ for a single random phase $\theta_i \sim \text{Uniform}(0, 1)$.

One boundary per step. The complete pseudocode of SHS is shown in Algorithm 1. When $p_{ik} \leq 1$ (as in DTMC kernels and in CTMC τ -leaping with sufficiently small h), at most one unit boundary can be crossed per step, so the `if` statement on Line 10 is sufficient. If an application allows $p_{ik} > 1$, the update should use an extra `while` loop to

Algorithm 1 Stratified Hazard Sampling (SHS) for CTMC/DTMC discrete generative models

```

1: Input:
2:   - Initial state  $X \sim p_0$ 
3:   - Time grid  $t_k = kh$  for  $k = 0, \dots, n$ 
4:   - A routine MODELSTEP( $t_k, X_{t_k}, i$ ) that returns:
5:     - change mass  $p_{ik} \in [0, 1]$ 
6:     - destination  $q_{k,i}(\cdot \mid X_{t_k})$ 
7:   (cf. (1), (2))
8: Output: Final sample  $X$  at  $t_n$  (i.e.,  $t = 1$ )
9: for  $i = 1$  to  $N$  do
10:   $S_i \leftarrow 0$ ;  $k_i \leftarrow 0$ ; Draw  $\theta_i \sim \text{Uniform}(0, 1)$ 
11: end for
12: for  $k = 0, 1, \dots, n - 1$  do
13:  for  $i = 1$  to  $N$  do
14:    $(p_{ik}, q_{k,i}) \leftarrow \text{MODELSTEP}(t_k, X_{t_k}, i)$ 
15:    $S_i \leftarrow S_i + p_{ik}$ 
16:   if  $S_i \geq \theta_i + k_i$  then /*crossed the next hazard
17:     boundary*/
18:      $X_{t_{k+1}}^i \sim q_{k,i}(\cdot \mid X_{t_k})$ 
19:      $k_i \leftarrow k_i + 1$ 
20:   else
21:      $X_{t_{k+1}}^i \leftarrow X_{t_k}^i$ 
22:   end if
23: end for
24: end for
25: return  $X_{t_n}$ 

```

handle multiple crossings.

Note that SHS changes only the *timing* of jump events by coupling the Bernoulli decisions across steps through a single phase θ_i . Importantly, SHS leaves the *destination sampling* $q_{k,i}$ unchanged, so the model’s categorical multimodality is preserved.

Jump-count concentration. Let $S_i^{\text{tot}} := S_{i,n} = \sum_{k=0}^{n-1} p_{ik}$ denote the total cumulative hazard/jump mass accumulated at position i . Write $S_i^{\text{tot}} = I_i + f_i$ with $I_i = \lfloor S_i^{\text{tot}} \rfloor$ and $f_i \in [0, 1)$. Since SHS counts how many thresholds $\theta_i + m$ are crossed by S_i^{tot} , we have

$$J_i = I_i + \mathbf{1}[\theta_i < f_i], \quad (9)$$

so $J_i \in \{I_i, I_i + 1\}$ and the long-tail jump-count fluctuations of step-wise Bernoulli sampling are eliminated. As a result, SHS suppresses the characteristic under-edit (too few substitutions) and over-edit (cascading substitutions) failure modes that arise under uniform-noise initialization.

4.1. Theoretical Properties

SHS is built on a simple primitive: *randomized rounding* of a nonnegative real mass S into an integer count $J \in \mathbb{Z}_{\geq 0}$

using a *single* uniform random variable. In SHS, this mass is the total cumulative hazard/jump mass S_i^{tot} at each position (Eq. (9)).

Proposition 4.1 (Unbiasedness). Fix $S \geq 0$ and draw $\theta \sim \text{Uniform}(0, 1)$. Let $\{S\} = S - \lfloor S \rfloor$ denote the fractional part and define $J = \lfloor S \rfloor + \mathbf{1}[\theta < \{S\}]$. Then $\mathbb{E}[J] = S$.

Proposition 4.2 (Minimal variance). With J as in Proposition 4.1, we have

$$\text{Var}(J) = \{S\}(1 - \{S\}) \leq \frac{1}{4}. \quad (10)$$

Moreover, among all integer-valued unbiased estimators of S supported on $\{\lfloor S \rfloor, \lceil S \rceil\}$, this variance is the minimum possible.

Proof sketch. Write $S = I + f$ with $I = \lfloor S \rfloor$ and $f = \{S\} \in [0, 1)$. Then $J = I + B$ where $B = \mathbf{1}[\theta < f] \sim \text{Bernoulli}(f)$. Hence $\mathbb{E}[J] = I + f = S$ and $\text{Var}(J) = f(1 - f) \leq 1/4$. See Appendix B for the full proof (and Appendix A for Proposition 4.1).

Interpretation. For a fixed mass S , standard step-wise simulation yields a Poisson-binomial count with variance $\sum_k p_k(1 - p_k)$, which can scale linearly with S in the many-edit regime. In contrast, SHS concentrates the count to two adjacent integers ($\lfloor S \rfloor$ or $\lceil S \rceil$), eliminating long-tail “sampler luck” in the number of edits while keeping the model’s categorical choices intact.

4.2. Lexically Constrained Safety via Phase-Allocated SHS

We consider blacklist-based lexical constraints, where users specify a forbidden token set $\mathcal{B} \subset \mathcal{V}$. Let the safe event be

$$\mathcal{A} = \{x \in \mathcal{V}^N : \forall i, x_i \notin \mathcal{B}\}. \quad (11)$$

Our goal is to approximate the conditional terminal distribution $p_1(x \mid \mathcal{A})$. As discussed in Section 2.2, exact conditioning corresponds to a Doob h -transform, which in general modifies both (i) *which* transitions are taken and (ii) *how frequently* they are taken. In contrast, naive masking modifies only the destination distribution and keeps the base jump frequency unchanged, often producing “late masking” artifacts.

Risk score. At time t and state x , we define a per-position violation risk score $r_i(t, x) \in [0, 1]$ as the forbidden mass under the (change-conditional) one-step proposal:

$$r_i(t, x) = \sum_{v \in \mathcal{B}} q_{t,i}(v \mid x), \quad (12)$$

where $q_{t,i}$ is the destination distribution conditional on changing the token (cf. (2) for DTMC kernels).

Algorithm 2 Safety-SHS with phase allocation (blacklist \mathcal{B})

```

1: Input: MODELSTEP routine (as in Algorithm 1); blacklist  $\mathcal{B}$ ; time grid  $t_k = kh$ ; initial state  $X \sim p_0$ 
2: Output: final sample  $X$  at  $t_n$  (i.e.,  $t = 1$ )
3: for  $i = 1$  to  $N$  do
4:    $S_i \leftarrow 0$ ;  $k_i \leftarrow 0$ ; Draw  $\theta_i^0 \sim \text{Uniform}(0, 1)$ 
5: end for
6: Compute severity scores and allocate phases at a reference step  $k_0$  (default  $k_0 = 0$ ).
7: for  $i = 1$  to  $N$  do
8:    $(p_{ik_0}, q_{k_0, i}) \leftarrow \text{MODELSTEP}(t_{k_0}, X_{t_{k_0}}, i)$ 
9:    $s_i(X) \leftarrow \mathbf{1}[X^i \in \mathcal{B}] + \sum_{v \in \mathcal{B}} q_{k_0, i}(v \mid X)$ 
10: end for
11: Assign phases  $\{\theta_i\}_{i=1}^N$  from  $\{\theta_i^0\}_{i=1}^N$  according to Eq. (14) using  $\{s_i(X)\}_{i=1}^N$ .
12: for  $k = 0, 1, \dots, n - 1$  do
13:   for  $i = 1$  to  $N$  do
14:      $(p_{ik}, q_{k, i}) \leftarrow \text{MODELSTEP}(t_k, X_{t_k}, i)$ 
15:      $S_i \leftarrow S_i + p_{ik}$ 
16:     if  $S_i \geq \theta_i + k_i$  then
17:       Sample  $X_{t_{k+1}}^i \sim q_{k, i}^{\text{MASK}}(\cdot \mid X_{t_k})$ 
18:        $k_i \leftarrow k_i + 1$ 
19:     else
20:        $X_{t_{k+1}}^i \leftarrow X_{t_k}^i$ 
21:     end if
22:   end for
23: end for
24: return  $X_{t_n}$ 

```

Phase timing without modifying base jump mass. Let $\theta_1^0, \dots, \theta_N^0 \stackrel{\text{i.i.d.}}{\sim} \text{Uniform}(0, 1)$ be *pre-sampled* SHS phases. We construct a *risk-to-phase assignment* that allocates smaller phases to higher-risk positions, thereby triggering earlier edits in cumulative hazard/jump-mass space while keeping the original per-position masses p_{ik} intact. That is, in the CTMC case, we keep $p_{ik} = h\lambda_i(t_k, x)$, while in the DTMC case, we keep $p_{ik} = 1 - P_{k,i}(x_i \mid x)$.

Given a reference time t_0 (default $t_0 = 0$) and state $x = X_{t_0}$, define a violation severity score

$$s_i(x) = \mathbf{1}[x_i \in \mathcal{B}] + r_i(t_0, x), \quad (13)$$

and let σ be a permutation such that $s_{\sigma(1)}(x) \geq \dots \geq s_{\sigma(N)}(x)$ (ties broken by index). Let $\theta_{(1)}^0 \leq \dots \leq \theta_{(N)}^0$ denote the ascending order statistics of $\{\theta_i^0\}_{i=1}^N$. We then assign

$$\theta_{\sigma(j)} \leftarrow \theta_{(j)}^0, \quad j = 1, \dots, N. \quad (14)$$

Thus, positions with larger violation severity receive smaller phase offsets, making their first SHS boundary (and hence first edit opportunity) occur earlier.

Masked destination (which transition). On a jump event at position i , we sample the new token from the masked destination

$$q_{t,i}^{\text{MASK}}(v \mid x) \propto q_{t,i}(v \mid x) \mathbf{1}[v \notin \mathcal{B}]. \quad (15)$$

Safety-SHS sampler (phase-allocated). We run the same SHS accumulation as Algorithm 1 with *unchanged* per-position jump mass p_{ik} , but we replace the i.i.d. phase initialization by the above phase allocation rule, and we sample destinations using q^{MASK} . This is a drop-in modification that does not require retraining and introduces no new continuous hyperparameters.

Effect on “late masking”. In SHS, the first jump at position i occurs when the cumulative mass $S_{i,k}$ crosses θ_i . By assigning smaller θ_i to high-risk positions, Safety-SHS resolves censorship-active positions earlier, reducing the failure mode where the rest of the sequence adapts to an unsafe token before it is removed. We validate this by measuring the time-to-first-safe-edit CDF and terminal distribution shift under censorship (Appendix D).

Remark (bias vs. conditioning). Unlike the rate-reweighting view of the Doob transform, phase allocation does not explicitly modify the base masses p_{ik} ; instead it biases the *relative event scheduling* across positions through the SHS phase offsets. Since our target under censorship is the *conditional* distribution $p_1(\cdot \mid \mathcal{A})$, some bias relative to the unconditional dynamics is expected and can be beneficial in mitigating late masking artifacts. Note that phase allocation breaks the i.i.d. Uniform phase initialization used in Propositions 4.1–4.2; accordingly, the unbiasedness guarantee is not intended to apply to the censored dynamics.

4.3. On Preserving Multi-modality: Decomposing Sampler Variance

A natural concern with our minimal-variance claim is whether reducing $\text{Var}(J_i)$ harms the multi-modality (generation diversity) that stochastic sampling aims to provide. We argue that SHS does not; instead, it selectively minimizes spurious variance from sampler instability while preserving meaningful variance from model expressiveness.

This can be formalized via the Law of Total Variance. Let $Q(X_1)$ denote the quality (e.g., likelihood or task metric) of a final sample X_1 at $t = 1$. The total variance in quality, $\text{Var}[Q(X_1)]$, arises from two sources of randomness: the sampling trajectory \mathcal{T} (controlled by SHS) and the model’s categorical choices \mathcal{U} at each jump (preserved by SHS). The

decomposition is:

$$\text{Var}[Q(X_1)] = \underbrace{\mathbb{E}_{\mathcal{T}}[\text{Var}_{\mathcal{U}}(Q(X_1) | \mathcal{T})]}_{\text{(Term 1: Model Expressiveness)}} + \underbrace{\text{Var}_{\mathcal{T}}[\mathbb{E}_{\mathcal{U}}(Q(X_1) | \mathcal{T})]}_{\text{(Term 2: Sampler Instability)}}.$$

Term 1 represents the “good” variance: the model’s inherent multi-modality in selecting diverse, high-quality tokens given a stable trajectory \mathcal{T} . SHS preserves this, as it does not modify the categorical sampling (Algorithm 1).

Term 2 represents the “bad” variance: instability from sampler “luck” in \mathcal{T} , leading to stuck (low J_i) or overshot (high J_i) paths with poor average quality $\mathbb{E}_{\mathcal{U}}[Q]$. This is not true diversity but unreliability.

SHS contributes by minimizing Term 2: bounding $\text{Var}(J_i) \leq 1/4$ ensures near-optimal paths ($J_i \approx I$ or $I+1$), driving $\text{Var}_{\mathcal{T}}[\mathbb{E}_{\mathcal{U}}(\cdot)]$ near zero. Thus, SHS enhances reliability without compromising the model’s expressive power.

5. Experiments

5.1. Setup

Our goal is to isolate the effect of *event-time sampling* on a continuous-time discrete generative model. Throughout this section, we keep the trained model (rate/velocity predictor) fixed and *only* change the sampling procedure: (i) the standard time-step Euler–Maruyama (EM) sampler, and (ii) our Stratified Hazard Sampling (SHS).

Few-step regime. To stress-test trajectory instability, we vary the number of discretization steps $n \in \{256, 64, 16, 8\}$ while keeping the same model and schedule.

5.2. Jump Timing Diagnostics in Hazard Space

We first validate whether SHS produces the intended *regularization of event times* without altering the per-jump categorical choice.

Let $\lambda(t)$ denote a (token-wise) jump rate along a sampled trajectory, and define the cumulative hazard

$$H(t) = \int_0^t \lambda(s) ds. \quad (16)$$

We record the hazard-space jump locations $\{H_k\}_{k \geq 1}$, where H_k is the cumulative hazard value at the k -th jump.

EM baseline: Erlang/Gamma-shaped locations. Under the standard NHPP view, inter-event increments in hazard space satisfy $\Delta H_k \sim \text{Exp}(1)$ i.i.d., so the k -th jump location

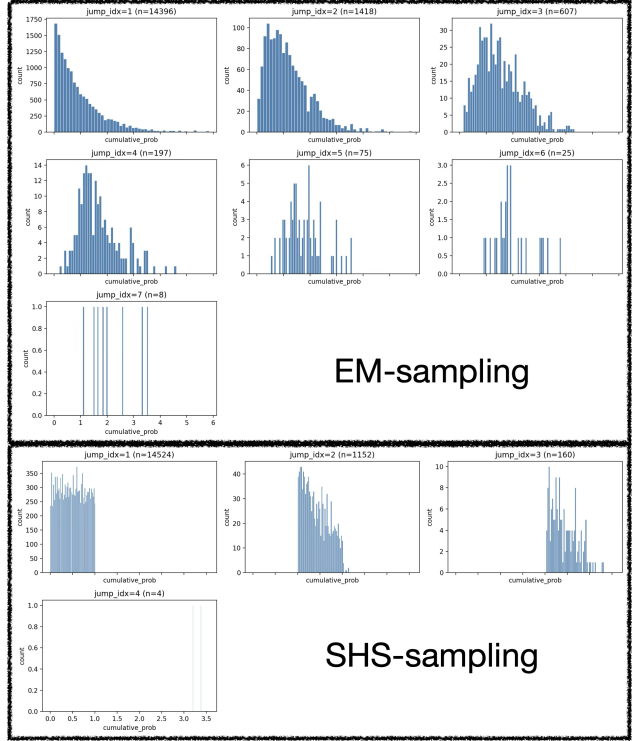


Figure 2. Hazard-space jump locations. Histograms of H_k (the cumulative hazard at the k -th jump). EM sampling exhibits Erlang/Gamma-shaped variability, while SHS produces stratified, bounded-support locations, demonstrating reduced trajectory randomness.

tion becomes

$$H_k = \sum_{i=1}^k \Delta H_i \sim \text{Gamma}(k, 1), \quad (17)$$

which yields an Erlang-shaped distribution as k increases. Empirically, we observe broad, heavy-tailed variability in early jump locations under EM sampling, consistent with the “under-/over-edit” instability in the noise-start setting.

SHS: stratified (bounded-support) jump locations. SHS triggers an event when the cumulative hazard crosses regularly spaced thresholds with a single random offset, which constrains the k -th event to occur within a narrow hazard interval (stratification). Consequently, the empirical histograms of H_k concentrate with bounded support and avoid the exponential long-tail behavior. This confirms that SHS makes the *timing* of jumps substantially more regular while leaving the per-jump destination sampling unchanged.

5.3. Quantized MNIST Reconstructions: Eliminating Under-Edit

We next visualize the practical effect of trajectory stabilization on a simple discrete generation task. Starting

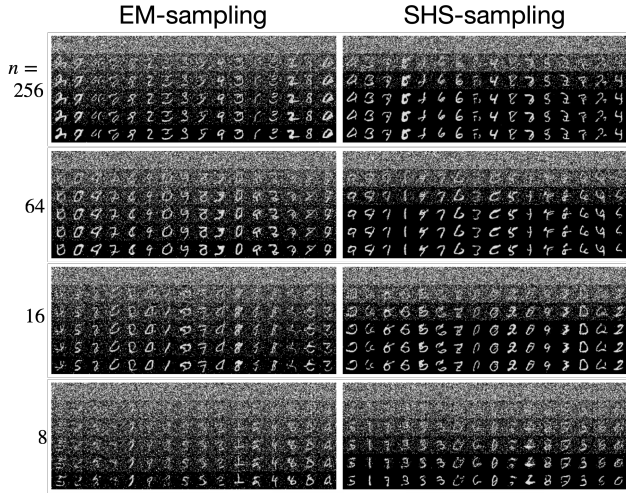


Figure 3. Quantized MNIST reconstructions under varying step budgets. EM vs. SHS at $n \in \{256, 64, 16, 8\}$ discretization steps. SHS reduces the under-edit regime and yields cleaner early-stage reconstructions.

from a noise initialization, we run the sampler for $n \in \{256, 64, 16, 8\}$ discretization steps and compare the resulting reconstructions.

Observation. EM sampling often exhibits an *under-edit* failure mode in the few-step regime: some positions experience too few jumps, leaving noticeable x_0 -derived noise even late in sampling. In contrast, SHS produces visibly cleaner samples at early stages and substantially reduces residual noise in low- n runs. Qualitatively, SHS maintains legible digit structure even at $n = 16$ and $n = 8$, where EM outputs remain dominated by unresolved noise.

5.4. UDLM Text Generation under Few-NFE Budgets

We next scale the same *sampler-only* ablation to a lightweight language-generation setting based on the UDLM evaluation protocol. As in all experiments, we keep the trained continuous-time discrete model (rate/velocity predictor) *fixed* and only swap the inference procedure between (i) the standard time-step Euler–Maruyama (EM) sampler and (ii) Stratified Hazard Sampling (SHS) (Schiff et al., 2025).

Protocol. For each compute budget $\text{NFE} \in \{4, 8, 16, 32, 64\}$, we generate 64 sentences per run and repeat the evaluation over 5 random seeds. We report (i) the sample entropy (as logged by the UDLM evaluation), and (ii) **generative perplexity (Gen. PPL)** computed by scoring the generated sentences using a fixed GPT2-large evaluator (lower is better).

NFE	EM		SHS	
	Entropy	Gen. PPL \downarrow	Entropy	Gen. PPL \downarrow
4	6.184 \pm 0.047	551.5 \pm 26.9	6.163 \pm 0.037	516.8 \pm 28.3
8	6.282 \pm 0.011	340.1 \pm 18.5	6.259 \pm 0.033	322.3 \pm 11.6
16	6.352 \pm 0.039	248.2 \pm 6.3	6.295 \pm 0.022	233.9 \pm 10.6
32	6.375 \pm 0.030	203.5 \pm 12.5	6.340 \pm 0.034	195.8 \pm 11.8
64	6.377 \pm 0.026	183.6 \pm 8.0	6.370 \pm 0.035	181.0 \pm 7.3

Table 1. UDLM text generation under NFE budgets. Mean \pm std over 5 seeds. Each run samples 64 sentences. Gen. PPL is computed by GPT2-large scoring (lower is better).

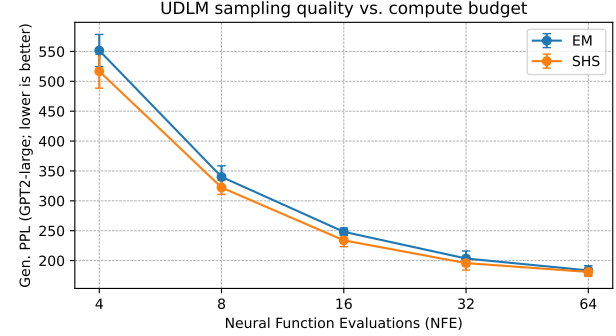


Figure 4. Gen. PPL vs. NFE (UDLM protocol). SHS improves generation quality most notably in the few-step regime, indicating reduced sampler-induced instability under tight compute budgets.

Results. Table 1 summarizes the mean and standard deviation over seeds, and Figure 4 plots Gen. PPL vs. NFE. SHS consistently improves Gen. PPL in the *few-step* regime, with the largest gains at very low NFE: at NFE=4/8/16/32, SHS reduces Gen. PPL by approximately 6.3%/5.2%/5.8%/3.8% relative to EM, respectively, while the gap narrows at NFE=64 (about 1.4%). This pattern is consistent with our claim that SHS primarily removes *sampler-induced trajectory variance* (irregular event timing / jump-count fluctuations), thereby mitigating under-edit behavior when the discretization budget is tight.

6. Conclusion

We proposed Stratified Hazard Sampling (SHS), a drop-in, hyperparameter-free variance-reduction rule for step-based inference in CTMC/DTMC discrete diffusion and flow models with a (stay vs. replace) structure. By stratifying cumulative hazard/jump mass with a single random phase per position, SHS preserves the expected number of edits while achieving minimal possible jump-count variance ($\leq 1/4$) without changing destination sampling.

Across quantized MNIST and a lightweight UDLM text-generation protocol, SHS improves stability and sample quality in the few-step / low-NFE regime. Future work will scale these findings to larger language/code benchmarks

and evaluate safety-oriented extensions such as lexically constrained sampling.

References

Austin, J., Johnson, D. D., Ho, J., Tarlow, D., and van den Berg, R. Structured denoising diffusion models in discrete state-spaces. In *Advances in Neural Information Processing Systems*, 2021.

Campbell, A., Benton, J., De Bortoli, V., Rainforth, T., Deligiannidis, G., and Doucet, A. A continuous time framework for discrete denoising models. In *Advances in Neural Information Processing Systems*, 2022.

Chang, H., Zhang, H., Jiang, L., Liu, C., and Freeman, W. T. Maskgit: Masked generative image transformer. In *Proceedings of the IEEE/CVF Conference on Computer Vision and Pattern Recognition (CVPR)*, 2022.

Dieleman, S., Sartran, L., Roshannai, A., Savinov, N., Ganin, Y., Richemond, P. H., Doucet, A., Strudel, R., Dyer, C., Durkan, C., et al. Continuous diffusion for categorical data. *arXiv preprint arXiv:2211.15089*, 2022.

Doob, J. L. Conditional brownian motion and the boundary limits of harmonic functions. *Bulletin de la Société Mathématique de France*, 85:431–458, 1957.

Gat, I., Remez, T., Shaul, N., Kreuk, F., Chen, R. T. Q., Synnaeve, G., Adi, Y., and Lipman, Y. Discrete flow matching. In *Advances in Neural Information Processing Systems (NeurIPS)*, 2024. URL <https://neurips.cc/virtual/2024/poster/95902>.

Gehman, S., Gururangan, S., Sap, M., Choi, Y., and Smith, N. A. RealToxicityPrompts: Evaluating neural toxic degeneration in language models. In Cohn, T., He, Y., and Liu, Y. (eds.), *Findings of the Association for Computational Linguistics: EMNLP 2020*, pp. 3356–3369, Online, November 2020. Association for Computational Linguistics. doi: 10.18653/v1/2020.findings-emnlp.301. URL <https://aclanthology.org/2020.findings-emnlp.301/>.

Ghazvininejad, M., Levy, O., Liu, Y., and Zettlemoyer, L. Mask-predict: Parallel decoding of conditional masked language models. *arXiv preprint arXiv:1904.09324*, 2019.

Grimmett, G. and Stirzaker, D. *Probability and Random Processes*. Oxford University Press, 4 edition, 2020. ISBN 9780198847601.

Han, X., Kumar, S., and Tsvetkov, Y. Ssd-lm: Semi-autoregressive simplex-based diffusion language model for text generation and modular control. *arXiv preprint arXiv:2210.17432*, 2022.

He, Z., Sun, T., Wang, K., Huang, X., and Qiu, X. Diffusionbert: Improving generative masked language models with diffusion models. In *Proceedings of the 61st Annual Meeting of the Association for Computational Linguistics (ACL)*, 2023.

Hokamp, C. and Liu, Q. Lexically constrained decoding for sequence generation using grid beam search. In Barzilay, R. and Kan, M.-Y. (eds.), *Proceedings of the 55th Annual Meeting of the Association for Computational Linguistics (Volume 1: Long Papers)*, pp. 1535–1546, Vancouver, Canada, July 2017. Association for Computational Linguistics. doi: 10.18653/v1/P17-1141. URL <https://aclanthology.org/P17-1141/>.

Hoogeboom, E., Nielsen, D., Jaini, P., Forré, P., and Welling, M. Argmax flows and multinomial diffusion: Learning categorical distributions. In *Advances in Neural Information Processing Systems*, 2021.

Hu, J. E., Khayrallah, H., Culkin, R., Xia, P., Chen, T., Post, M., and Van Durme, B. Improved lexically constrained decoding for translation and monolingual rewriting. In Burstein, J., Doran, C., and Solorio, T. (eds.), *Proceedings of the 2019 Conference of the North American Chapter of the Association for Computational Linguistics: Human Language Technologies, Volume 1 (Long and Short Papers)*, pp. 839–850, Minneapolis, Minnesota, June 2019. Association for Computational Linguistics. doi: 10.18653/v1/N19-1090. URL <https://aclanthology.org/N19-1090/>.

Lewis, P. A. W. and Shedler, G. S. Simulation of nonhomogeneous poisson processes by thinning. *Naval Research Logistics Quarterly*, 26(3):403–413, 1979. doi: 10.1002/nav.3800260304.

Lou, A., Meng, C., and Ermon, S. Discrete diffusion modeling by estimating the ratios of the data distribution. In *Proceedings of the 41st International Conference on Machine Learning (ICML)*, 2024.

Post, M. and Vilar, D. Fast lexically constrained decoding with dynamic beam allocation for neural machine translation. In Walker, M., Ji, H., and Stent, A. (eds.), *Proceedings of the 2018 Conference of the North American Chapter of the Association for Computational Linguistics: Human Language Technologies, Volume 1 (Long Papers)*, pp. 1314–1324, New Orleans, Louisiana, June 2018. Association for Computational Linguistics. doi: 10.18653/v1/N18-1119. URL <https://aclanthology.org/N18-1119/>.

Rao, V. and Teh, Y. W. Fast MCMC sampling for markov jump processes and continuous-time bayesian networks. *Journal of Machine Learning Research*, 14:3295–3320, 2013.

Rogers, L. C. G. and Williams, D. *Diffusions, Markov Processes, and Martingales: Volume 2, Itô Calculus*. Cambridge University Press, 2000.

Ross, S. M. *Introduction to Probability Models*. Academic Press, 13 edition, 2023.

Schiff, Y., Sahoo, S. S., Phung, H., Wang, G., Rush, A., Kuleshov, V., Dalla-Torre, H., Boshar, S., de Almeida, B. P., and Pierrot, T. Simple guidance mechanisms for discrete diffusion models. In *International Conference on Learning Representations (ICLR)*, 2025.

A. Full Proof of Proposition 4.1 (Unbiasedness)

We restate the proposition in the scalar form. Fix $S \geq 0$ and draw $\theta \sim \text{Uniform}(0, 1)$. Let $I = \lfloor S \rfloor$ and $f = \{S\} = S - I \in [0, 1)$. Define

$$J = I + \mathbf{1}[\theta < f].$$

Then

$$\mathbb{E}[J] = I + \mathbb{P}(\theta < f) = I + f = S,$$

since θ is uniform on $[0, 1]$. This proves Proposition 4.1.

B. Full Proof of Proposition 4.2 (Minimal Variance)

Using the notation from Appendix A, we have $J = I + B$ where $B = \mathbf{1}[\theta < f] \sim \text{Bernoulli}(f)$. Since I is deterministic,

$$\text{Var}(J) = \text{Var}(I + B) = \text{Var}(B) = f(1 - f) \leq \frac{1}{4},$$

where the last inequality follows because the quadratic $f(1 - f)$ attains its maximum at $f = 1/2$.

Minimality among two-point unbiased estimators. Any integer-valued random variable \tilde{J} supported on $\{I, I + 1\}$ is determined by $p = \mathbb{P}(\tilde{J} = I + 1)$. Unbiasedness $\mathbb{E}[\tilde{J}] = S = I + f$ forces $p = f$. Therefore $\text{Var}(\tilde{J}) = p(1 - p) = f(1 - f)$ for any such unbiased estimator, and SHS attains this minimum. This proves Proposition 4.2.

C. Additional Analysis of Stratified Hazard Sampling

This appendix collects additional properties of Stratified Hazard Sampling (SHS) and clarifies its scope for CTMC/DTMC-based samplers.

C.1. SHS as a systematic coupling of Bernoulli trials

Consider a fixed sequence of per-step change masses $\{p_k\}_{k=0}^{n-1} \subset [0, 1]$ and define the cumulative sums $S_k = \sum_{j=0}^{k-1} p_j$ (with $S_0 = 0$) and $S_n = \sum_{k=0}^{n-1} p_k$. The standard step-based sampler draws independent indicators $B_k^{\text{iid}} \sim \text{Bernoulli}(p_k)$ and the total number of changes is $J = \sum_k B_k^{\text{iid}}$ (Poisson-binomial).

SHS instead draws a *single* phase $\theta \sim \text{Uniform}(0, 1)$ and defines a coupled indicator sequence by

$$B_k^{\text{shs}} = \mathbf{1}[\lfloor S_k \rfloor + \mathbf{1}[\theta < \{S_k\}] < \lfloor S_k + p_k \rfloor + \mathbf{1}[\theta < \{S_k + p_k\}]], \quad (18)$$

which is equivalent to triggering a change whenever the cumulative sum crosses the next unit boundary $\theta + m$. Summing (18) over k yields the randomized-rounding form $J^{\text{shs}} = \lfloor S_n \rfloor + \mathbf{1}[\theta < \{S_n\}]$ (cf. Eq. (9)).

C.2. Event-time stratification in cumulative hazard space

For a CTMC with an *exogenous* (state-independent) rate $\lambda(t) \geq 0$, define the continuous cumulative hazard $S(t) = \int_0^t \lambda(\tau) d\tau$. SHS places event boundaries at $\theta, \theta + 1, \theta + 2, \dots$ in hazard space, so the m -th event time is

$$T_m = \inf\{t \in [0, 1] : S(t) \geq \theta + (m - 1)\}. \quad (19)$$

Equivalently, the hazard value at event m is exactly $\theta + (m - 1)$. Thus, SHS guarantees *exactly one* event in each unit-length hazard interval, eliminating the exponential-tail inter-arrival variability of Poisson processes in hazard space (where $\Delta S \sim \text{Exp}(1)$).

On a discrete grid (DTMC kernels or CTMC τ -leaping), S_k increases in steps. If each increment satisfies $p_k \leq p_{\max} \leq 1$, then the boundary-crossing event triggered at step k overshoots its hazard boundary by at most p_{\max} . Therefore, SHS still yields tightly controlled event locations in hazard/jump-mass space even under discretization.

C.3. Scope: inference-time variance reduction vs. exact simulation

The results in Propositions 4.1–4.2 are unconditional statements about randomized rounding for a *fixed* mass S (or a fixed sequence $\{p_k\}$). In a full generative model, the per-step masses $p_{ik}(x)$ (or rates $\lambda_i(t, x)$) are typically *state-dependent*. Because SHS couples change decisions over time through the phase θ_i , it introduces additional memory beyond the visible state x . Accordingly, SHS should be viewed as an *inference-time variance reduction integrator* for CTMC/DTMC samplers rather than as an exact simulator of the underlying Markov process.

Despite this, SHS leaves the per-change destination kernels $q_{k,i}$ untouched and dramatically reduces sampler-induced variability in the number and timing of edits. This reduction is especially valuable under uniform-noise initialization, where meaningful generation requires multiple self-correction edits per position and where Poisson-binomial fluctuations can dominate the observed instability.

D. Safety Evaluation Details

This appendix details the evaluation protocol used to support the claim in Section 4.2 that our *phase allocation* reduces the distributional mismatch to the conditional target $p_1(\cdot | A)$ compared to naive masking.

D.1. Setup and Compared Samplers

Lexical constraint. Let \mathcal{V} be the vocabulary and $\mathcal{B} \subset \mathcal{V}$ a blacklist. The safe set is

$$\mathcal{A} = \{x \in \mathcal{V}^N : \forall i, x_i \notin \mathcal{B}\}. \quad (20)$$

The ideal constrained target distribution is the conditional terminal distribution $p_1(x | \mathcal{A}) \propto p_1(x) \mathbf{1}[x \in \mathcal{A}]$ (cf. Eq. (5) in the main text). We compare:

- **Unconstrained:** baseline sampler without any censorship.
- **Mask-only (naive):** at each jump, sample from the masked destination $q_{t,i}^{\text{MASK}}(v | x) \propto q_{t,i}(v | x) \mathbf{1}[v \notin \mathcal{B}]$, while keeping the original escape rates $\lambda_i(t, x)$ unchanged.
- **Mask + phase allocation (ours):** same masked destination as above, but allocate SHS phases $\{\theta_i\}$ by assigning smaller pre-sampled phases to higher-risk positions (Section 4.2, Eq.(14)), while keeping the original escape rates $\lambda_i(t, x)$ unchanged.
- **Rejection reference (optional):** samples from the unconstrained sampler followed by rejection of sequences not in \mathcal{A} , used as an empirical proxy for $p_1(\cdot | \mathcal{A})$ (Section D.4).

Why the reference is meaningful. Since $p_1(x | \mathcal{A}) \propto p_1(x) \mathbf{1}[x \in \mathcal{A}]$, acceptance–rejection from p_1 yields exact conditional samples when the base sampler is exact, and provides a practical approximation otherwise. We report the acceptance rate to contextualize how challenging the constraint is.

D.2. Risk Score and Safety-Critical Edits

Our method accelerates positions that are likely to be affected by censorship. To make this measurable, we define a *pre-mask risk score* from the model’s unfiltered destination distribution.

Pre-mask forbidden mass. Given the current state x at time t , define for each position i :

$$r_i(t, x) = \sum_{v \in \mathcal{B}} q_{t,i}(v | x), \quad (21)$$

where $q_{t,i}(\cdot | x)$ is computed *before* applying the blacklist filter. Intuitively, $r_i(t, x)$ estimates how much the unconstrained dynamics “wants” to place a forbidden token at position i at time t .

Safety-critical (censorship-active) jump. We call a jump at position i and time t *safety-critical* if

$$r_i(t, X_{t-}) \geq \tau, \quad (22)$$

for a fixed threshold $\tau \in (0, 1)$. This focuses the analysis on edits where masking materially changes the local transition. In all safety experiments, we report τ and include a sensitivity check over a small grid (e.g., $\tau \in \{0.01, 0.05, 0.1\}$).

Remark (robust variant). If the initial distribution p_0 can contain blacklisted tokens, we additionally mark an edit as safety-critical whenever $X_{t^-}^i \in \mathcal{B}$, since such a token must eventually be removed to satisfy \mathcal{A} .

D.3. Time-to-First-Safe-Edit CDF

To quantify the “late masking” failure mode, we measure how early the sampler performs a safety-critical edit under each censorship method.

Definition. Let $\{t_k\}_{k=0}^n$ be the discretization times ($t_k = kh$). For a sampled trajectory $(X_{t_k})_{k=0}^n$, define the *time-to-first-safe-edit*

$$T_{\text{edit}} = \min \left\{ t_k : \exists i \text{ such that a jump occurred at } (i, t_k) \text{ and } r_i(t_k, X_{t_k^-}) \geq \tau \right\}, \quad (23)$$

with the convention $T_{\text{edit}} = 1$ if no such edit occurs.

Empirical CDF. Given M independent runs, we estimate

$$\widehat{F}_{\text{edit}}(t) = \frac{1}{M} \sum_{m=1}^M \mathbf{1}[T_{\text{edit}}^{(m)} \leq t]. \quad (24)$$

We plot $\widehat{F}_{\text{edit}}(t)$ for Mask-only vs. Ours. A left-shift (larger CDF at the same t) indicates that safety-critical positions are resolved earlier, consistent with our claim that phase allocation mitigates late masking.

Optional complementary curves. We also report: (i) *time-to-last-safe-edit* T_{last} (the last time a safety-critical jump occurs), and (ii) the *unsafe survival curve* $t \mapsto \mathbb{P}(\exists i : r_i(t, X_t) \geq \tau)$, both of which directly diagnose “late” censorship activity.

D.4. Approximating $p_1(\cdot \mid \mathcal{A})$ by Rejection

When feasible, we build a reference set of samples approximating $p_1(\cdot \mid \mathcal{A})$ via rejection:

1. Run the **Unconstrained** sampler to produce terminal samples $x^{(1)}, x^{(2)}, \dots$
2. Accept samples with $x^{(m)} \in \mathcal{A}$ until collecting M_{ref} accepted samples.

We denote the resulting empirical reference distribution by \widehat{p}_{ref} . We report the acceptance rate $\hat{\alpha} = M_{\text{ref}}/M_{\text{drawn}}$.

Practical note. If $\hat{\alpha}$ is too small for a given blacklist, we (i) shorten the generated length, (ii) use a milder blacklist, or (iii) treat the reference as approximate and rely on the two-sample metrics in Section D.5 without claiming exactness.

D.5. Terminal Distribution Shift Induced by Censorship

We quantify how much censorship distorts the terminal distribution relative to the conditional target. Let $\mathcal{S}_{\text{ref}} = \{x_{\text{ref}}^{(m)}\}_{m=1}^{M_{\text{ref}}}$ be the rejection reference and $\mathcal{S}_{\text{meth}} = \{x_{\text{meth}}^{(m)}\}_{m=1}^M$ be samples produced by a censorship method (Mask-only or Ours). We report multiple complementary discrepancy measures.

(1) Per-position token marginal JSD. For each position i , define empirical marginals

$$\hat{p}_i^{\text{ref}}(v) = \frac{1}{M_{\text{ref}}} \sum_{m=1}^{M_{\text{ref}}} \mathbf{1}[x_{\text{ref},i}^{(m)} = v], \quad \hat{p}_i^{\text{meth}}(v) = \frac{1}{M} \sum_{m=1}^M \mathbf{1}[x_{\text{meth},i}^{(m)} = v]. \quad (25)$$

We compute the Jensen–Shannon divergence

$$\text{JSD}_i = \text{JSD}(\hat{p}_i^{\text{meth}} \parallel \hat{p}_i^{\text{ref}}), \quad \text{JSD}(p \parallel q) = \frac{1}{2} \text{KL}\left(p \parallel \frac{p+q}{2}\right) + \frac{1}{2} \text{KL}\left(q \parallel \frac{p+q}{2}\right), \quad (26)$$

and report the average $\frac{1}{N} \sum_{i=1}^N \text{JSD}_i$.

(2) Sequence-level feature divergence. To capture higher-order effects beyond position-wise marginals, we additionally compute a divergence on lightweight sequence features $\phi(x)$, such as: (i) unigram/bigram count vectors, or (ii) a fixed pretrained sentence embedding. For count-based features, we compute JSD between normalized feature histograms. For embeddings, we report a kernel two-sample statistic (MMD) or a linear-probe classification accuracy (two-sample test) as a proxy for distributional shift.

Interpretation. Smaller discrepancy to \hat{p}_{ref} indicates closer approximation to $p_1(\cdot \mid A)$. We expect Mask-only to incur larger shift because it only filters one-step destinations (Eq. (8)) and does not capture the lookahead-dependent scheduling effects implied by the Doob h -transform (Eq. (7)). In contrast, our *phase allocation* prioritizes early edits at high-risk positions, reducing late masking artifacts and the resulting terminal distribution shift.